Membrane Cholesterol Regulates the Oligomerization and Fusogenicity of SARS-CoV Fusion Peptide: Implications in Viral Entry

Geetanjali Meher[†,‡], Surajit Bhattacharjya[§]* and Hirak Chakraborty[†,¶]*

[†]School of Chemistry, Sambalpur University, Jyoti Vihar, Burla, Odisha 768 019, India
[¶]Centre of Excellence in Natural Products and Therapeutics, Sambalpur University, Jyoti Vihar, Burla, Odisha 768 019, India
[§] School of Biological Sciences, Nanyang Technological University, 60 Nanyang Drive, Singapore 637551

*Address correspondence to Hirak Chakraborty, E-mail: hirak@suniv.ac.in or Surajit Bhattacharjya, Email: surajit@ntu.edu.sg

[‡]Present Address: School of Biological Sciences, National Institute of Science Education and Research, Bhubaneswar, India

ESI contains the methods section.

ABSTRACT

N-terminal residues (770–788) of the S2 glycoprotein of severe acute respiratory syndrome coronavirus (SARS-CoV), has been recognized as a potential fusion peptide that can be involved in entry of the virus into the host cell. Membrane composition plays an important role in lipid-peptide interaction and the oligomeric status of the peptide. SARS-CoV fusion peptide (S2 fusion peptide) is known to undergo cholesterol-dependent oligomerization in membrane; however, its significance in membrane fusion is still speculative. This study aimed to investigate the oligomerization of SARS-CoV fusion peptide in a membrane containing phosphatidylcholine, phosphatidylethanolamine, and phosphatidylglycerol, with varying concentrations of cholesterol, and to evaluate peptide-induced membrane fusion to correlate the importance of peptide oligomerization with membrane fusion. Peptide-induced modulation of membrane organization and dynamics was explored by steady-state and time-resolved fluorescence spectroscopic measurements using depth-dependent probes. Results clearly demonstrated the induction of S2 fusion peptide oligomerization by membrane cholesterol and the higher efficiency of oligomer in promoting membrane fusion compared to that of its monomeric counterpart. Cholesterol-dependent peptide oligomerization and membrane fusion are important aspects of viral infection, since the cholesterol level can change with age as well as with the onset of various pathophysiological conditions.

INTRODUCTION

Severe acute respiratory syndrome (SARS) is a highly infectious form of pneumonia caused by coronaviruses (CoVs). The global outbreak of SARS had been limited to approximately 8098 cases, resulting in 774 deaths in 29 countries, till July 2003.[1, 2] However, the current pandemic caused by SARS-CoV-2 is unprecedented in terms of infectivity of the virus. According to Johns Hopkins University database, more than 6 million people have died due to the pandemic while approximately half a billion more are affected; this necessitates a better understanding of the pathogenesis of this virus.[3] SARS-CoVs form a group of large enveloped RNA viruses capable of causing respiratory, hepatic, and enteric diseases. The spike protein (S) present in the envelope catalyzes entry of the virion into the host cell. The S protein of SARS-CoV has two proteolytic domains, namely S1 and S2. The binding of S1 domain to the angiotensin-converting enzyme (ACE2) receptor on the cell surface leads to cleavage of the S protein, thereby initiating conformational changes in the S2 domain.[4, 5] The latter then exposes 20–25 N-terminal residues, known as the SARS-CoV fusion peptide, which directly interacts with the host cell membrane, and facilitates the fusion process. Besides the N-terminal fusion peptide (FP), the S2 subunit contains multiple internal fusion peptides, unlike other class I viral fusion proteins.[6] The S2 protein contains two heptad regions (HR1 and HR2) and a transmembrane (TM) region at the C-terminus (Scheme-1). While the entry of SARS-CoV is largely believed to occur via fusion of the virion with the cell membrane,[7] an alternative mechanism of endocytosis-mediated cellular internalization followed by fusion with the endosome at low pH has also been proposed.[8]

Contrary to that of other class I viral fusion peptides, the exact location, and sequence of coronavirus fusion peptides are still elusive. Several putative fusion peptide sequences have been proposed in recent years based on biophysical and syncytia formation results.[9-16] The immediate

downstream peptide of the S2 cleavage site of the spike protein is also suggested as a probable fusion peptide sequence by several groups.[17-19] The uncertainty regarding the exact sequence of fusion peptide could be an inherent characteristic of the SARS-CoV fusion peptide itself. In other words, the cell fusion process of SARS viruses could involve multiple fusion peptides with potential synergistic activity.[10] The N-terminal fusion peptide of SARS CoV, investigated in this work, was identified by Wimley and co-workers,[12] and those of SARS-CoV-1 and SARS-CoV-2 were found to be identical, except for position-1, which is methionine in the former and isoleucine in the latter.[20] The diagnostic activity of FP in the fusion of model membranes was delineated. Further, a scrambled sequence of FP was found to be inactive in fusogenic assays. This peptide demonstrated significant hemolytic and hemagglutinating activities, both being greater than that of SFIEDLLFNKVTLADAGFGGGKKKK.[16] Previous studies with other class I fusion peptides, such as those of influenza hemagglutinin and HIV-1 gp41, had demonstrated the correlation of hemolytic and hemagglutinating activities of synthetic peptides with their ability to promote membrane fusion.[21-23] This fusion peptide displays strong affinity toward membranes and implicated in membrane fusion.[9, 24] Moreover, the N-terminal fusion peptides from other class I viruses have been shown to promote membrane fusion.[25] NMR measurements have shown the S2 fusion peptide to assume a bent α-helical structure in DPC micelles[24] while tending to assume β-sheet conformation in lipid membranes.[26] The S2 fusion peptide has higher binding affinity towards negatively charged membranes, owing to its formal charge of +2 at physiological pH.[9] Cryo-EM-derived structure of S fusion protein suggested a six-helix bundle topology with trimeric fusion peptide region in a post-fusion conformation.[27] X-ray crystallographic structures of the S2 domain of S protein, largely focusing on HR1, HR2, and HR1/HR2 complex, confirmed canonical trimeric coiled-coil helical structures akin to type I fusion system.[6] However, mechanistic

information regarding S2 protein oligomerization and host cell membrane fusion is still mostly lacking. This study aimed to demonstrate cholesterol-dependent oligomerization of S2 fusion peptide in model membranes using homo-Fluorescence Resonance Energy Transfer (homo-FRET). The fusion peptide did not oligomerize in POPC/POPG (80/20 mol%) membrane until a high peptide concentration (peptide-to-lipid ratio 0.1) was achieved; however, oligomerization did occur at lower concentration of peptide in the membrane containing 10 or 20 mol% cholesterol.[28] Direct correlation between oligomerization and fusion, however, remains to be elucidated.

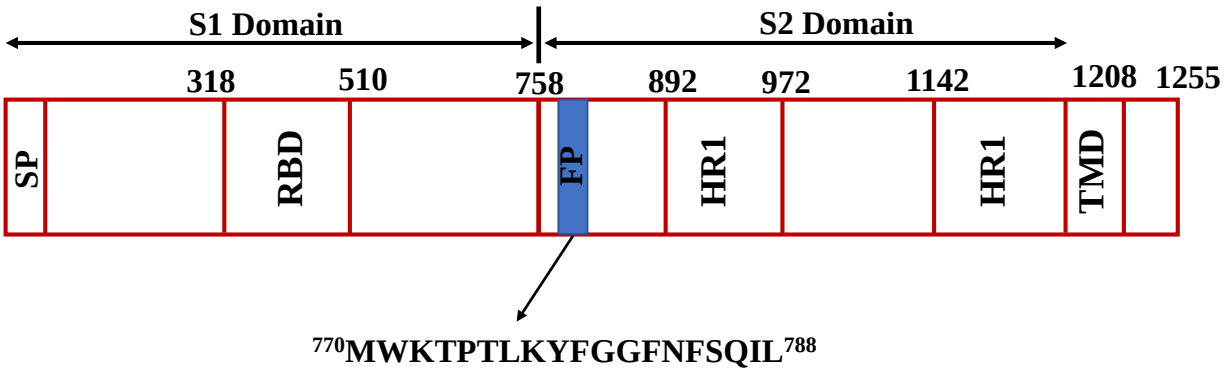

Scheme 1. Spike glycoprotein of SARS-CoV is constituted of S1 and S2 domains separated by a protease cleavage site. The fusion peptide (FP) locates at the N-terminal of S2 domain. The figure has been adapted and modified from reference 29.

In this study, we selected a fusogenic lipid composition of DOPC/DOPE/DOPG, and explored the oligomerization of S2 fusion peptide, along with its effect on membrane organization and dynamics, as well as fusion. Identical measurements were performed in membranes containing 10 and 20 mol% cholesterol to evaluate the effect of membrane cholesterol on peptide oligomerization and membrane fusion. Cholesterol is known to enhance stability and reduce permeability of the membrane.[30] The unique arrangement of cholesterol inside the lipid bilayer induces steric interactions with lipid acyl chains, thereby modulating the physical properties of the membrane.[31, 32] Further, cholesterol is associated with successful entry of both influenza virus[33] and SARS-

CoV-2[34] into the host cell. Recently published clinical data have shown the administration of statin, a cholesterol reducing drug, to be associated with a better clinical outcome and significant reduction of mortality risk in patients with COVID-19.[35] Computational studies have predicted possible binding of statin to multiple target proteins of SARS-CoV-2.[36] The higher infectivity and risk of COVID-19 in the aged population may be due to higher cholesterol levels in the elderly.[37] Therefore, evaluation of the effect of cholesterol on fusion of host cell membrane with SARS viruses would be of particular importance.

The current study further highlighted the role of phosphatidyl ethanolamine (PE) in peptide organization. Phosphatidylethanolamine (PE) is a zwitterionic phospholipid present in the outer leaflet of cell membranes, and plays an important role in membrane fusion as well as disassembly of the contractile ring during cytokinesis in cell division.[38, 39] Moreover, PE causes an intrinsic negative curvature in the membrane due to its inverted cone-shaped molecular structure, similar to cholesterol.[40, 41] X-ray diffraction results had demonstrated that PE helps in reducing the energy for stalk-like state formation, which is believed to be an early fusion intermediate.[42, 43] In addition, PE enhances the rates of lipid mixing and content mixing in any lipid composition.[40] Therefore, evaluation of the oligomerization status of S2 fusion peptide in PC/PE/PG membranes would allow evaluation of the plausible role of PE in peptide oligomerization. In this study, we have extensively utilized multiple steady-state and time-resolved fluorescence techniques to understand the role of cholesterol and PE in the oligomerization of S2 fusion peptide as well as its impact on membrane fusion. Overall, our study would contribute to a better understanding of the importance of fusion peptide oligomerization in membrane fusion vis-à-vis viral entry.

Materials and Methods

Materials

Cholesterol (CH), 1,2-dioleoyl-*sn*-glycero-3-phosphocholine (DOPC), 1,2-dioleoyl-*sn*-glycero-3-phosphoethanolamine (DOPE), and chloroform stock solutions of 1,2-dioleoyl-*sn*-glycero-3-phospho-(1'-*rac*-glycerol) (sodium salt) (DOPG) were purchased from Avanti Polar Lipids (Alabaster, AL). NBD-PE, Rh-PE, DPH and TMA-DPH were procured from Invitrogen (Eugene, OR). We have purchased Terbium chloride and N-[tris(hydroxymethyl) methyl]2-2-aminoethane sulfonic acid (TES) from Alfa Aeser (Haverhill, MA). Dipicolinic acid (DPA), Sephadex G-75, Triton X-100 (TX-100) and PEG of molecular weight 7000–9000 (PEG 8000) were obtained from Sigma Aldrich (St. Louis, MO). Calcium chloride and sodium chloride were obtained from Merck, India, and Fisher Scientific (India), respectively. Ethylenediaminetetraacetic acid (EDTA) and Spectroscopic grade DMSO were purchased from Spectrochem (India). The S2 fusion peptide (M^{770}WKTPTLKYFGGFNFSQIL) was chemically synthesized and purified by GL-Biochem (China) with a purity of >98%. All other chemicals used in the work were of the highest available purity. Water was purified through Millipore (Bedford, MA) Milli-Q water purification system. *Please see the Supplementary Information for methods.*

Results and discussion

Lipid composition modulates the fusogenicity of fusion peptide by altering its structure,[44] oligomeric status,[45] and ability of membrane penetration.[28] On the other hand, binding of the peptide to the membrane,[45, 46] and peptide-induced alteration in membrane organization and dynamics depend on lipid composition.[47, 48] It has been shown earlier by Weliky group that the chemical synthesized trimer of gp41 fusion peptide assumes β-sheet conformation in membranes

containing cholesterol, and demonstrates higher rate and extent of lipid mixing compared to its monomeric and dimeric counterparts.[49, 50] On the contrary, association of the same trimeric peptide displays a mixture of helical and β-strand conformation in membranes without cholesterol.[49] The membrane proximal region of gp41 fusion peptide further shows cholesterol-dependent membrane fusion.[51] In our earlier study, the S2 fusion peptide from SARS-CoV (M^{770}WKTPTLKYFGGFNFSQIL^{788}) had been shown to oligomerize in POPC/POPG membranes in a cholesterol-dependent manner.[45] Moreover, the peptide promotes stalk formation in DOPC/DOPE/DOPG (60/30/10 mol%) membranes in absence of PEG.[9] In this study, we explored the interaction of S2 fusion peptide with a PE-containing lipid membrane, DOPC/DOPE/DOPG (50/30/20 mol%), and evaluated effect of the peptide on fusion. Amount of phosphatidylcholine was systematically substituted by cholesterol up to 20 mol% to assess the cholesterol dependency of membranotropic and fusogenic properties of the peptide. This strategy provided us the opportunity to study the propensity of cholesterol-dependent oligomerization of S2 fusion peptide, and elucidate the effect of peptide oligomerization on membrane fusion process. Steady-state and time-resolved fluorescence techniques were employed to understand the effect of peptide binding and peptide oligomerization on membrane organization and dynamics. Moreover, we evaluated fusion efficacy of the peptide in lipid compositions mentioned above to correlate peptide oligomerization with membrane fusion.

Peptide oligomerization in membranes: role of phosphatidylethanolamine and cholesterol

Fluorescence anisotropy is commonly employed to evaluate the occurrence of homo-FRET.[52] Fluorophores with relatively smaller Stokes shift transfer excited state energies to other identical fluorophores that are in ground state.[53] This process of deactivation of excited fluorophores is

known as homo-FRET. Homo-FRET always leads to depolarization of emitted light, since dipoles of the excited and absorbing fluorophores do not resemble each other, resulting in reduction of fluorescence anisotropy.[52, 54]

We had previously utilized homo-FRET of tryptophan to evaluate the oligomerization of fusion peptide of SARS-CoV spike protein in POPC/POPG membranes.[45] Similarly, in this study, we measured fluorescence anisotropy of the single tryptophan, present in the fusion peptide of SARS-CoV spike protein, at varying concentrations of the peptide in DOPC/DOPE/DOPG membranes, and in presence of 10 and 20 mol% cholesterol (**Figure 1**). Fluorescence anisotropy of tryptophan decreased with increasing peptide concentrations in all three lipid compositions (0, 10, and 20 mol% cholesterol). However, the change was remarkably sharp in the membrane containing 20 mol% cholesterol. The decrease in tryptophan fluorescence anisotropy could be attributed to homo-FRET of the fluorophore resulting from oligomerization of the fusion peptide. Propensity of oligomerization of the fusion peptide was much higher in the membrane containing 20 mol% cholesterol than in that containing 0 or 10 mol% cholesterol. It is pertinent to mention here that the high fluorescence anisotropy value of Trp at the lowest peptide concentration in the presence of the 20 mol% cholesterol is attributed to the membrane ordering ability of cholesterol. The rigid ring structure of cholesterol reduces the *transgauche* isomerization of the neighboring lipid acyl chains, and thereby orders them resulting in a reduction of their dynamics and fluidity.[55] Interestingly, we did not observe any oligomerization in the absence of cholesterol in POPC/POPG membranes till the peptide-to-lipid ratio of 0.045;[45] however, a significant drop in tryptophan fluorescence anisotropy was observed in DOPC/DOPE/DOPG membranes at a relatively lower peptide-to-lipid ratio (0.02), indicating the occurrence of oligomerization even in the absence of cholesterol. This scenario may be ascribed to the presence of phosphatidylethanolamine in the

membrane. Interestingly, both phosphatidylethanolamine and cholesterol promote negative curvature of the membrane,[41] which raises the question of whether negative curvature of the membrane would facilitate oligomerization of fusion peptide. The trimeric structure of S fusion protein[56] and the lipid-induced negative curvature[41, 55, 57] are known to promote membrane fusion. Moreover, the lipid envelope of influenza virus contains higher amount of phosphatidylethanolamine than most mammalian cells,[58] and cholesterol content of human immunodeficiency virus is much higher than that of the host cell.[51, 59, 60] Therefore, the role of phosphatidylethanolamine in inducing S peptide oligomerization could be thought-provoking, since fusion might be facilitated via the simultaneous effect of protein oligomerization and negative curvature generation.

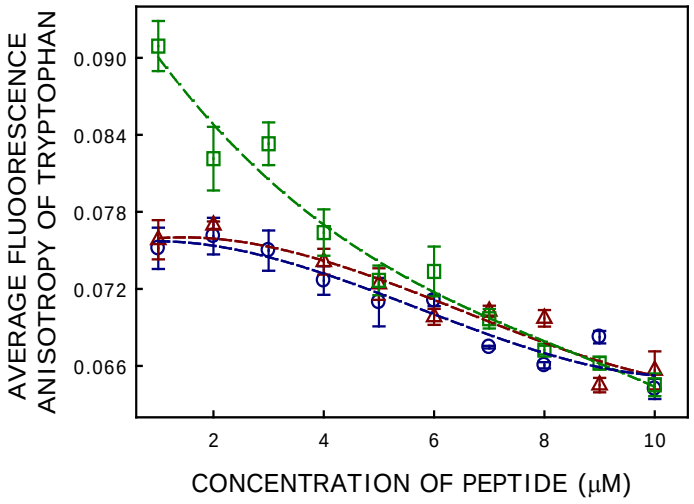

Figure 1. Change in average fluorescence anisotropy of tryptophan with varying concentration of DOPC/DOPE/DOPG (50/30/20 mol%) (Blue, o), DOPC/DOPE/DOPG/CH (40/30/20/10 mol%) (Red, Δ) and DOPC/DOPE/DOPG/CH (30/30/20/20 mol%) (Green, □) membranes. All measurements were carried out in 10 mM TES, 100 mM NaCl, 1mM CaCl2 and 1 mM EDTA at pH 7.4 and 37 ºC. The concentration of lipid was kept constant at 200 μM and the emission was monitored at 350 nm by exciting at 295 nm. See the Methods section in Supplementary Information for more details.

Effect of SARS-CoV fusion peptide on the hydrophobic order of membranes

The hydrophobic probe DPH is exploited for the measurement of rotational flexibility of long acyl chains of the membrane. DPH is a rod-like molecule, localized approximately 7.8 Å from the center of the bilayer.[61] Fluorescence anisotropy of DPH was measured as a function of peptide concentration both in absence and presence of cholesterol (**Figure 2**). DPH anisotropy increased significantly in presence of lower concentrations of peptide, and reached a saturation at a peptide concentration of 2 μM (P/L = 0.01). The peptide-induced change in DPH anisotropy (Δr) dropped appreciably with increasing concentration of membrane cholesterol. The estimated value of Δr was 0.023 in the cholesterol-depleted membrane, whereas it reduced to 0.009 in the 20 mol% cholesterol-containing membrane. This indicated that the fusion peptide penetrated deeper into DOPC/DOPE/DOPG membranes, and the depth of penetration might be reduced in cholesterol-containing membranes. Considering the higher propensity of the peptide to oligomerize in cholesterol-containing membrane, either the monomeric peptide displayed deeper penetration compared to its oligomeric counterpart or cholesterol-induced rigidification of the membrane was detrimental to the deep penetration of fusion peptide.

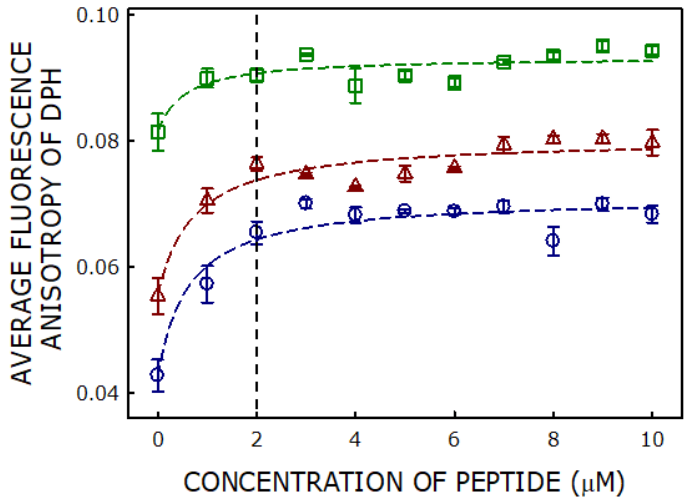

Figure 2. Plot of average fluorescence anisotropy of DPH with varying concentration of SARS-CoV fusion peptide in DOPC/DOPE/DOPG (50/30/20 mol%) (Blue, o), DOPC/DOPE/DOPG/CH

(40/30/20/10 mol%) (Red, Δ) and DOPC/DOPE/DOPG/CH (30/30/20/20 mol%) (Green, □) membranes. All measurements were carried out in 10 mM TES, 100 mM NaCl, 1mM $CaCl_2$ and 1 mM EDTA at pH 7.4 and 37 ºC. The concentration of lipid and DPH were kept constant at 200 μM and 1 μM, respectively. The emission was monitored at 428 nm by exciting at 360 nm. See the Methods section in Supplementary Information for more details.

Effect of SARS-CoV fusion peptide on polarity of the hydrophobic region of membranes

Fluorescence lifetime is used to measure the polarity around a probe in a micro-heterogeneous environment. Change in fluorescence lifetime of DPH in membranes was used to monitor the peptide-induced change in polarity around the hydrophobic region of the membrane (**Figure 3**). Although there was no significant change in the fluorescence lifetime of DPH in presence of the fusion peptide in 20 mol% cholesterol-containing membranes, the peptide did alter polarity of the hydrophobic region of the membrane to a small extent in presence of 0 and 10 mol% cholesterol composition at higher peptide concentrations. This could be attributed to differential penetration of the peptide in membranes containing varying amounts of cholesterol.

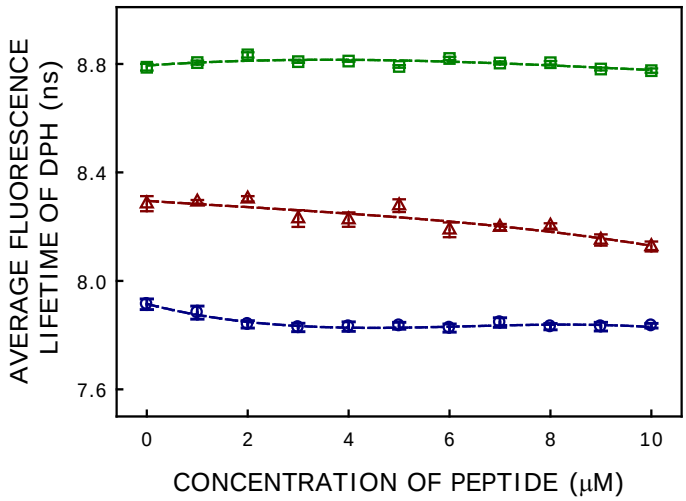

Figure 3. Plot of mean fluorescence lifetime of DPH with varying concentration of SARS-CoV fusion peptide in DOPC/DOPE/DOPG (50/30/20 mol%) (BLUE, o), DOPC/DOPE/DOPG/CH (40/30/20/10 mol%) (RED, Δ) and DOPC/DOPE/DOPG/CH (30/30/20/20 mol%) (GREEN, □) membranes. All measurements were carried out in 10 mM TES, 100 mM NaCl, 1mM $CaCl_2$ and 1 mM EDTA at pH 7.4 and 37 ºC. The concentration of lipid and DPH were kept constant at 200 μM and 1μM, respectively. The emission was monitored at 428 nm by exciting at 338 nm. See the Methods section in Supplementary Information for more details.

Effect of SARS-CoV fusion peptide on the interfacial region of membranes

The trimethylammonium derivative of DPH (TMA-DPH) is known to be located at the interfacial region of the bilayer with an average distance of 10.9Å from the center of the bilayer.[61] Rotational flexibility of the interfacial region could be monitored by measuring the fluorescence anisotropy of TMA-DPH. The latter is shown in **Figure 4** in presence of various concentrations of S2 fusion peptide in different membranes. TMA-DPH anisotropy displayed peptide-dependent small alterations in the membranes containing 0 and 10 mol% cholesterol, whereas no significant change was observed in the 20 mol% cholesterol-containing membrane. The result indicated that interfacial packing of the 0 and 10 mol% cholesterol-containing membranes is partially affected in presence of higher concentrations of S2 fusion peptide, although it was not so for the 20 mol% cholesterol-containing membranes.

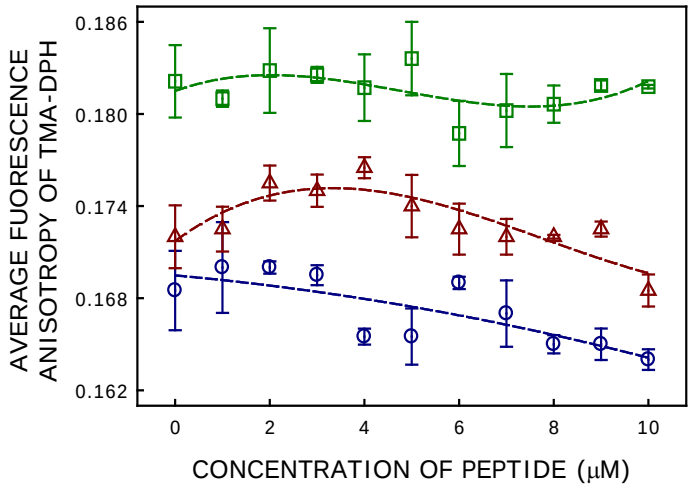

Figure 4. Plot of average fluorescence anisotropy of TMA-DPH with varying concentration of SARS-CoV fusion peptide in DOPC/DOPE/DOPG (50/30/20 mol%) (BLUE, o), DOPC/DOPE/DOPG/CH (40/30/20/10 mol%) (RED, Δ) and DOPC/DOPE/DOPG/CH (30/30/20/20 mol%) (GREEN, □) membranes. All measurements were carried out in 10 mM TES, 100 mM NaCl, 1mM $CaCl_2$ and 1 mM EDTA at pH 7.4 and 37 ºC. The concentration of lipid and TMA-DPH were kept constant at 200 μM and 1μM, respectively. The emission was monitored at 428 nm by exciting at 360 nm. See the Methods section in Supplementary Information for more details.

Effect of SARS-CoV fusion peptide on polarity of the interfacial region of membranes

Fluorescence lifetime of TMA-DPH was measured to evaluate peptide-dependent change in membrane interfacial polarity (Figure 5). Fluorescence lifetime of TMA-DPH increased with increase in peptide concentration in the membrane. The fusion peptide showed a significant change in peptide-dependent polarity of the interfacial region of membranes in all three lipid compositions. However, the change was more pronounced in membranes containing 20 mol% cholesterol (0.73 ns in presence of 10 μM peptide). Since the peptide was majorly oligomeric in 20 mol% cholesterol-containing membranes, the oligomer was considered to displace water molecules (highly polar) from the interfacial region of the membrane, thereby reducing the effective water concentration at the interfacial region. Peptide-induced drying of interfacial region has been conjectured to promote membrane aggregation and stalk formation.[62, 63] The change in TMA-DPH fluorescence lifetime was relatively small in the membranes containing 0 and 10 mol% cholesterol, probably implying lesser displacement of water from the membrane interface, hence explaining the low propensity of peptide oligomerization.

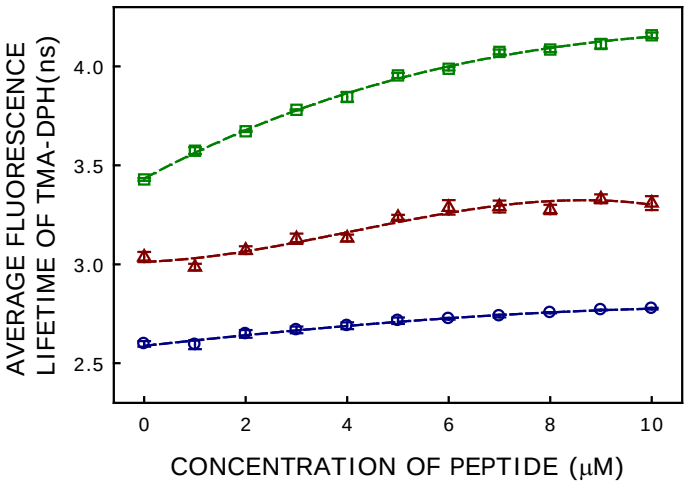

Figure 5. Plot of mean fluorescence lifetime of TMA-DPH with varying concentration of SARS-CoV fusion peptide in DOPC/DOPE/DOPG (50/30/20 mol%) (Blue, o), DOPC/DOPE/DOPG/CH (40/30/20/10 mol%) (Red, Δ) and DOPC/DOPE/DOPG/CH (30/30/20/20 mol%) (Green, □)

membranes. All measurements were carried out in 10 mM TES, 100 mM NaCl, 1mM $CaCl_2$ and 1 mM EDTA at pH 7.4 and 37 ºC. The concentration of lipid and DPH were kept constant at 200 μM and 1μM, respectively. The emission was monitored at 428 nm by exciting at 338 nm. See the Methods section in Supplementary Information for more details.

Depth of penetration of the SARS-CoV fusion peptide in membranes

The depth of penetration of the fusion peptide was estimated by measuring FRET efficiency of tryptophan with TMA-DPH and DPH, as discussed in the Methods section, and the results are shown in **Figure 6**. Location of the lone tryptophan could be estimated from the ratio of FRET efficiency of tryptophan with TMA-DPH to that with DPH [E_T(TMA-DPH)/E_T(DPH)]. Higher value of the ratio was indicative of closeness of tryptophan to TMA-DPH (shallow penetration), whereas lower ratio indicated deeper penetration of tryptophan . Our results reported the FRET ratio to increase with increase in cholesterol concentration in the membrane. In DOPC/DOPE/DOPG (50/30/20 mol%) membranes, the FRET efficiency ratio was found to be 1.31, whereas in DOPC/DOPE/DOPG/CH (40/30/20/10 mol%) and in DOPC/DOPE/DOPG/CH (30/30/20/20 mol%) membranes, the ratios were 1.42 and 1.48, respectively. The finding suggested that the tryptophan was majorly located at the interfacial region (ratio is greater than 1); however, the exact location would depend on the cholesterol content of the membrane. It penetrated relatively deeper in the membrane when the membrane lacked cholesterol, whereas it moved upward (shallow penetration) in membranes containing cholesterol. This result corroboated with those of DPH anistropy.

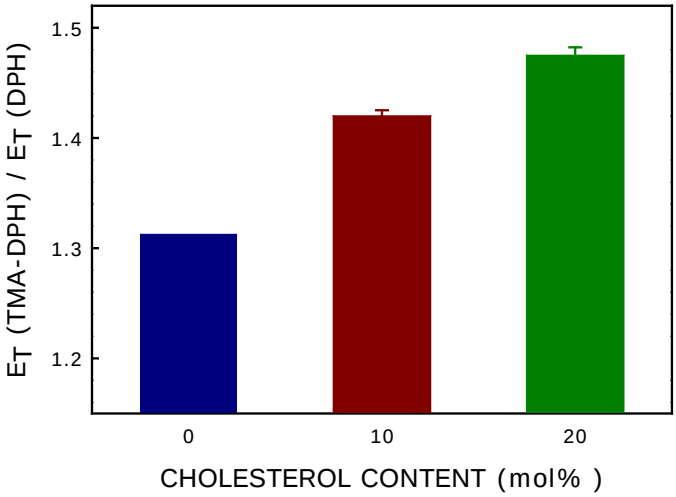

Figure 6. Plot of FRET efficiency of tryptophan with TMA-DPH and DPH, E_T(TMA-DPH)/E_T(DPH), of SARS-CoV fusion peptide in DOPC/DOPE/DOPG (50/30/20, mol%) (blue), DOPC/DOPE/DOPG/CH (40/30/20/10, mol%) (red) and DOPC/DOPE/DOPG/CH (30/30/20/20, mol%) (green) membranes. The lipid concentration was kept constant at 200 µM and peptide concentration was fixed at 2 µM. The TMA-DPH and DPH concentrations are kept constant at 2 µM. All measurements were carried out in 10 mM TES, 100 mM NaCl, 1mM $CaCl_2$ and 1 mM EDTA at pH 7.4 and 37 ºC. All measurements are average of at least three independent measurements. See the Methods section in Supplementary Information for more details.

Effect of SARS-CoV on PEG-mediated vesicle fusion

Polyethylene glycol (PEG)-mediated membrane fusion is a well-established fusion model for evaluating the effect of peptide and other membranotropic peptides on fusion.[64-68] In this study, we used 6% (w/v) PEG to induce vesicle fusion, and evaluated the effect of S2 fusion peptide on PEG-mediated fusion. Such low concentrations of PEG had previously been shown to have no influence on the tryptophan fluorescence intensity, binding mode, affinity, and physical state of the peptide.[46, 69, 70] Time courses of lipid mixing (LM), content mixing (CM), and content leakage (L) were measured during the PEG-mediated SUV fusion of 0, 10, and 20 mol% cholesterol-containing membranes using the methodologies described in the Methods section. Vesicular fusion induced by PEG alone was considered as the control, and the effect of peptide (measured in presence of both peptide and PEG) was compared with it. The peptide-to-lipid ratio was kept

constant at 0.01 to maintain the physiological significance of peptide concentration.[71] **Figures 7 (A-C)** show the time courses of lipid mixing, content mixing, and content leakage both in absence and presence of S2 fusion peptide in DOPC/DOPE/DOPG membranes. The percentage of LM, CM and L were calculated using equations 2, 3, and 4, respectively (see Methods section in supplementary information). The extents of lipid mixing, content mixing, and content leakage at infinite time were estimated by fitting the lines of Figures 6 (A-C) to an exponential equation using SigmaPlot (San Jose, CA) software package, and the results are shown in Table-1. The rate constant values of lipid mixing have also been calculated from the fitting of the time-dependent lipid mixing data in single exponential equation. The extent of lipid mixing provides the information of maximum amount of intermixing of lipids in a particular system, whereas rate constant offers the promptness of the process. Content mixing provides the information of mixing of contents between two vesicles; whereas content leakage is a measurement of spontaneous leakage of probes from the vesicles. Content leakage is parameter associated to the integrity of the membrane.

Table 1. Extent and Rate Constant of Lipid Mixing in the presence of SARS-CoV Fusion Peptide

Lipid Composition (200 μM)	Peptide (2 μM)	Lipid Mixing (%)	κ (sec^{-1})
DOPC/DOPE/DOPG (50/30/20)	Control	2.6	ND
	S2 fusion peptide	25.5	1.27×10^{-3}
DOPC/DOPE/DOPG/CH (40/30/20/10)	Control	1.1	ND
	S2 fusion peptide	35.2	1.65×10^{-3}
DOPC/DOPE/DOPG/CH (30/30/20/20)	Control	3.5	ND
	S2 fusion peptide	48.9	1.97×10^{-3}

Similar measurements were performed for the fusion of membranes containing 10 and 20 mol% cholesterol to evaluate the effect of membrane cholesterol vis-à-vis peptide oligomerization on membrane fusion. **Figures 7(D-F) and Figures 7(G-I)** represent the time courses of lipid mixing, content mixing, and content leakage for membranes containing 10 and 20 mol% cholesterol, respectively.

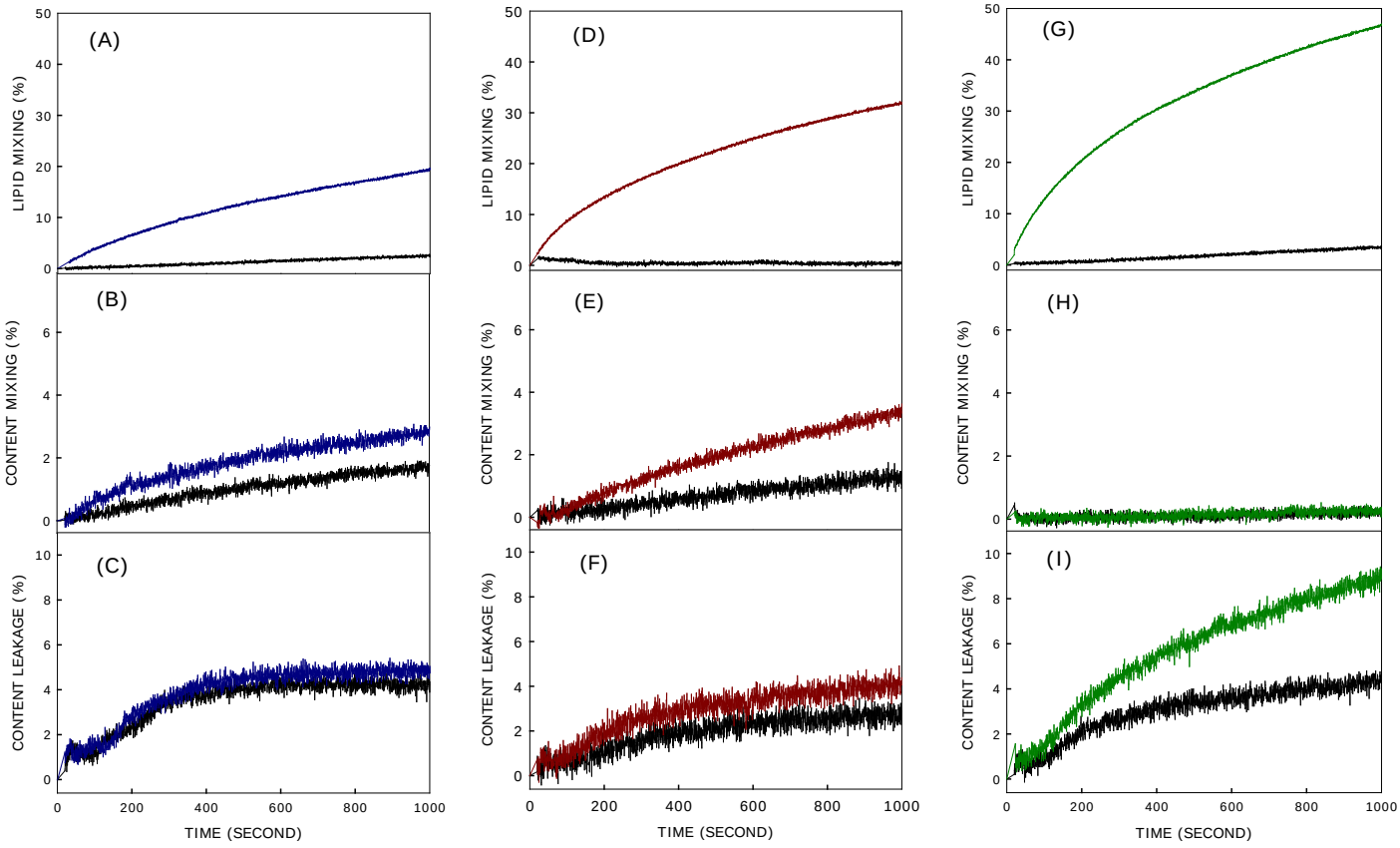

Figure 7. Effect of S2 fusion peptide on the lipid mixing, content mixing and content leakage of membranes containing 0, 10 and 20 mol% cholesterol. A, D, G represent the kinetics of PEG-mediated lipid mixing in absence (control, black lines) and in presence of S2 fusion peptide in DOPC/DOPE/DOPG (50/30/20 mol%) (blue), DOPC/DOPE/DOPG/CH (40/30/20/10 mol%) (red), and DOPC/DOPE/DOPG/CH (30/30/20/20 mol%) (green) membranes. Similar color codes have been used for the kinetics of content mixing (B, E and H) and content leakage (C, F and I). The membrane fusion was induced by 6 weight% of PEG at 37 ºC. Results are shown for a peptide to lipid ratio of 0.01. All measurements were carried out in 10 mM TES, 100 mM NaCl, 1mM $CaCl_2$ and 1 mM EDTA, pH 7.4 at a total lipid concentration of 200 µM. The representative data

is the average of at least three independent measurements. See the Methods section in Supplementary Information for more details.

In all membrane compositions, S2 fusion peptide had significant effect on lipid mixing, without much influence on content mixing, in PEG-mediated membrane fusion (**Figure 7)**. The peptide displayed enhanced rate and extent of lipid mixing with increasing membrane cholesterol. However, the maximum content mixing is less than 4% for all three membranes despite significant amount of lipid mixing. Almost 0% content mixing for the membrane containing 20 mol% cholesterol could be attributed to the relatively higher leakage value in this system, as leakage lowers the signal for content mixing due to the release of Tb^{3+} and DPA from the respective trapped volume. The percentage of lipid mixing increased from 25% to 49% upon increasing membrane cholesterol from 0 to 20 mol% (**Table 1**), whereas the rate of lipid mixing was enhanced by approximately 1.6-fold. The same peptide induced 3.5% lipid mixing in DOPC/DOPE/DOPG (60/30/10 mol%) in absence of PEG, whereas the value went up to 11.5% in DOPC/DOPE/DOPG/CH (40/30/10/20 mol%) membranes.[20] The extent was much higher in PEG-mediated fusion, since PEG promoted aggregation and dehydration of membranes favouring a facile fusion. However, the N-terminal fusion peptide of S protein was incapable of promoting content mixing; the lower content leakage (less than 10%) ensured integrity of the membrane under all conditions. According to the classical stalk model of membrane fusion, lipid mixing is majorly associated with the formation of 'stalk' and 'transmembrane contact,' whereas content mixing represents pore opening. Our results indicated that while the S2 fusion peptide promotes stalk and transmembrane contact formation, it cannot open the pore between two apposed membranes. Moreover, the extent of intermediate formation was found to be directly correlated with the cholesterol content of the membrane. A recent work by Zaccai and co-workers has shown using

neutron scattering experiments that the structure and function of fusion peptides of SARS-CoV-2 spike protein depend on the cholesterol content of the membrane.[11] Oligomerization of peptide was directly associated with membrane cholesterol; the peptide was majorly monomeric at a peptide-to-lipid ratio of 0.01 (fusion experiments were carried at this peptide to lipid ratio), and the extent of oligomerization increased with increasing membrane cholesterol. The extent and rate of peptide-induced stalk formation (lipid mixing) was enhanced by approximately 2-, and 1.6-fold in the membrane containing 20 mol% cholesterol compared to that in the membrane devoid of cholesterol. The increase in rate and extent of fusion was positively correlated with oligomerization of the peptide.

Oligomerization of fusion protein from class I viruses is well documented.[72-74] Even the spike protein of SARS-CoV-2 was found to be trimeric.[75] Therefore, oligomerization of fusion protein is considered to be an important aspect of activation of membrane fusion process. Our results further supported the higher functional ability of oligomeric fusion peptide over its monomeric counterpart. Interestingly, S2 fusion peptide is incapable of pore opening, which is contrary to other fusion peptides from class I viruses.[66] This could be the plausible reason for the existence of multiple fusion peptides in SARS-coronaviruses, which might be working synergistically towards pore opening.

Conclusions

Our results clearly demonstrated that the N-terminal fusion peptide of S protein from SARS-CoV oligomerizes in DOPC/DOPE/DOPG (60/30/10 mol%) membranes even at a peptide-to-lipid ratio higher than 0.01, and the propensity of oligomerization enhances with increasing concentration of membrane cholesterol. In our previous work in POPC/POPG (80/20 mol%) membranes, we had

not observed any detectable peptide aggregation until a very high concentration of peptide (peptide-to-lipid ratio 0.04) was added to the membrane; however, the oligomerization occurred at lower peptide concentration when the membrane contained 10 or 20 mol% cholesterol.[45] Comparison of these two results led us to explore the role of phosphatidylethanolamine (PE) in inducing aggregation of S2 fusion peptide. Both cholesterol and PE have intrinsic negative curvature.[41] Therefore, lipids with intrinsic negative curvature may be considered to play an important role in peptide oligomerization. Oligomerization is a general theme for class I viral fusion proteins.[56] Our fusion results demonstrated that enhancement of the extent and rate of lipid mixing are parallel to the oligomerization of S2 fusion peptide. However, the S2 fusion peptide is incapable of pore opening,[20] contrary to that reported for hemagglutinin fusion peptide, even in presence of PEG.[66] Therefore, the role of N-terminal fusion peptide of S protein is different from that of other class I viral fusion peptides. The synergistic effect of multiple fusion peptides in S protein might be instrumental in pore opening, and necessitates a detailed study in future.

Author Contributions

H.C conceptualized the work, analyzed the data, and wrote the final manuscript, S.B conceptualized the work and wrote the final manuscript, and G.M carried out all the experiments, analyzed the data, and wrote the initial draft of the manuscript.

Conflicts of interest

There are no conflicts to declare.

Acknowledgement

This work was supported by Core Research Grant (CRG/2021/001515) of Science and Engineering Research Board (SERB), and SERB-Science and Technology Award for Research (STR/2021/000029), Department of Science and Technology (DST), New Delhi to HC, and

Ministry of Education (MOE), Singapore to SB. HC thanks the University Grants Commission for UGC-Assistant Professor position. HC and GM thank DST, New Delhi and UGC for providing the instrument facility to the School of Chemistry, Sambalpur University under the FIST and DRS programs, respectively. We thank members of Chakraborty laboratory for their comments and discussions.

References

1. B. Sainz, Jr., J. M. Rausch, W. R. Gallaher, R. F. Garry and W. C. Wimley, *Biochemistry*, 2005, **44**, 947-958.
2. H. Hofmann and S. Pohlmann, *Trends Microbiol*, 2004, **12**, 466-472.
3. A. G. Harrison, T. Lin and P. Wang, *Trends Immunol*, 2020, **41**, 1100-1115.
4. S. A. Jeffers, S. M. Tusell, L. Gillim-Ross, E. M. Hemmila, J. E. Achenbach, G. J. Babcock, W. D. Thomas, Jr., L. B. Thackray, M. D. Young, R. J. Mason, D. M. Ambrosino, D. E. Wentworth, J. C. Demartini and K. V. Holmes, *Proc Natl Acad Sci U S A*, 2004, **101**, 15748-15753.
5. W. Li, M. J. Moore, N. Vasilieva, J. Sui, S. K. Wong, M. A. Berne, M. Somasundaran, J. L. Sullivan, K. Luzuriaga, T. C. Greenough, H. Choe and M. Farzan, *Nature*, 2003, **426**, 450-454.
6. H. Chakraborty and S. Bhattacharjya, *Biophys Chem*, 2020, **265**, 106438.
7. S. Belouzard, J. K. Millet, B. N. Licitra and G. R. Whittaker, *Viruses*, 2012, **4**, 1011-1033.
8. H. Wang, P. Yang, K. Liu, F. Guo, Y. Zhang, G. Zhang and C. Jiang, *Cell Res*, 2008, **18**, 290-301.
9. J. Guillen, R. F. de Almeida, M. Prieto and J. Villalain, *J Phys Chem B*, 2008, **112**, 6997-7007.
10. J. Guillen, P. K. Kinnunen and J. Villalain, *Biochim Biophys Acta*, 2008, **1778**, 2765-2774.
11. A. Santamaria, K. C. Batchu, O. Matsarskaia, S. F. Prévost, D. Russo, F. Natali, T. Seydel, I. Hoffmann, V. Laux, M. Haertlein, T. A. Darwish, R. A. Russell, G. Corucci, G. Fragneto, A. Maestro and N. R. Zaccai, *Journal of the American Chemical Society*, 2022, **144**, 2968-2979.
12. B. Sainz, Jr., J. M. Rausch, W. R. Gallaher, R. F. Garry and W. C. Wimley, *J Virol*, 2005, **79**, 7195-7206.
13. I. G. Madu, S. L. Roth, S. Belouzard and G. R. Whittaker, *J Virol*, 2009, **83**, 7411-7421.
14. C. M. Petit, J. M. Melancon, V. N. Chouljenko, R. Colgrove, M. Farzan, D. M. Knipe and K. G. Kousoulas, *Virology*, 2005, **341**, 215-230.
15. R. K. Koppisetti, Y. G. Fulcher and S. R. Van Doren, *J Am Chem Soc*, 2021, **143**, 13205-13211.
16. L. G. M. Basso, A. E. Zeraik, A. P. Felizatti and A. J. Costa-Filho, *Biochim Biophys Acta Biomembr*, 2021, **1863**, 183697.
17. R. N. Kirchdoerfer, C. A. Cottrell, N. Wang, J. Pallesen, H. M. Yassine, H. L. Turner, K. S. Corbett, B. S. Graham, J. S. McLellan and A. B. Ward, *Nature*, 2016, **531**, 118-121.
18. A. C. Walls, M. A. Tortorici, B. J. Bosch, B. Frenz, P. J. M. Rottier, F. DiMaio, F. A. Rey and D. Veesler, *Nature*, 2016, **531**, 114-117.
19. A. L. Lai, J. K. Millet, S. Daniel, J. H. Freed and G. R. Whittaker, *J Mol Biol*, 2017, **429**, 3875-3892.
20. G. P. Pattnaik, S. Bhattacharjya and H. Chakraborty, *Biochemistry*, 2021, **60**, 559-562.
21. P. W. Mobley, H. F. Lee, C. C. Curtain, A. Kirkpatrick, A. J. Waring and L. M. Gordon, *Biochim Biophys Acta*, 1995, **1271**, 304-314.
22. P. W. Mobley, A. J. Waring, M. A. Sherman and L. M. Gordon, *Biochim Biophys Acta*, 1999, **1418**, 1-18.
23. S. A. Wharton, S. R. Martin, R. W. Ruigrok, J. J. Skehel and D. C. Wiley, *J Gen Virol*, 1988, **69 (Pt 8)**, 1847-1857.
24. M. Mahajan and S. Bhattacharjya, *Biochim Biophys Acta*, 2015, **1848**, 721-730.
25. B. Apellániz, N. Huarte, E. Largo and J. L. Nieva, *Chem Phys Lipids*, 2014, **181**, 40-55.
26. M. Mahajan, D. Chatterjee, K. Bhuvaneswari, S. Pillay and S. Bhattacharjya, *Biochim Biophys Acta Biomembr*, 2018, **1860**, 407-415.
27. J. Shang, G. Ye, K. Shi, Y. Wan, C. Luo, H. Aihara, Q. Geng, A. Auerbach and F. Li, *Nature*, 2020, **581**, 221-224.
28. G. Meher, S. Sinha, G. P. Pattnaik, S. Ghosh Dastidar and H. Chakraborty, *J Phys Chem B*, 2019, DOI: 10.1021/acs.jpcb.9b04577.
29. B. J. Bosch, R. van der Zee, C. A. de Haan and P. J. Rottier, *J Virol*, 2003, **77**, 8801-8811.

30. S. Raffy and J. Teissie, *Biophys J*, 1999, **76**, 2072-2080.
31. N. Kucerka, J. Pencer, M. P. Nieh and J. Katsaras, *Eur Phys J E Soft Matter*, 2007, **23**, 247-254.
32. J. Pan, T. T. Mills, S. Tristram-Nagle and J. F. Nagle, *Phys Rev Lett*, 2008, **100**, 198103.
33. K. N. Liu and S. G. Boxer, *Biophys J*, 2021, **120**, 4832-4841.
34. D. W. Sanders, C. C. Jumper, P. J. Ackerman, D. Bracha, A. Donlic, H. Kim, D. Kenney, I. Castello-Serrano, S. Suzuki, T. Tamura, A. H. Tavares, M. Saeed, A. S. Holehouse, A. Ploss, I. Levental, F. Douam, R. F. Padera, B. D. Levy and C. P. Brangwynne, *eLife*, 2021, **10**.
35. V. Castiglione, M. Chiriacò, M. Emdin, S. Taddei and G. Vergaro, *European heart journal. Cardiovascular pharmacotherapy*, 2020, **6**, 258-259.
36. D. Ghosh, D. Ghosh Dastidar, K. Roy, A. Ghosh, D. Mukhopadhyay, N. Sikdar, N. K. Biswas, G. Chakrabarti and A. Das, *Sci Rep*, 2022, **12**, 6241.
37. H. Chakraborty, *Current Science*, 2020, **118**, 1157.
38. T. Atsumi, E. Matsuura and T. Koike, in *Systemic Lupus Erythematosus (Fourth Edition)*, ed. R. G. Lahita, Academic Press, San Diego, 2004, DOI: https://doi.org/10.1016/B978-012433901-9/50042-9, pp. 1081-1105.
39. K. Emoto, T. Kobayashi, A. Yamaji, H. Aizawa, I. Yahara, K. Inoue and M. Umeda, *Proc Natl Acad Sci U S A*, 1996, **93**, 12867-12872.
40. M. E. Haque, T. J. McIntosh and B. R. Lentz, *Biochemistry*, 2001, **40**, 4340-4348.
41. H. T. McMahon and E. Boucrot, *Journal of cell science*, 2015, **128**, 1065-1070.
42. D. P. Siegel and R. M. Epand, *Biophys J*, 1997, **73**, 3089-3111.
43. L. Chernomordik, *Chem Phys Lipids*, 1996, **81**, 203-213.
44. A. L. Lai, A. E. Moorthy, Y. Li and L. K. Tamm, *J Mol Biol*, 2012, **418**, 3-15.
45. G. Meher, S. Bhattacharjya and H. Chakraborty, *J Phys Chem B*, 2019, **123**, 10654-10662.
46. G. P. Pattnaik and H. Chakraborty, *Chem Phys Lipids*, 2018, **217**, 35-42.
47. G. Meher and H. Chakraborty, *J Membr Biol*, 2019, DOI: 10.1007/s00232-019-00064-7

10.1007/s00232-019-00064-7 [pii].
48. G. Meher and H. Chakraborty, *Chem Phys Lipids*, 2021, **234**, 105025.
49. W. Qiang and D. P. Weliky, *Biochemistry*, 2009, **48**, 289-301.
50. R. Yang, M. Prorok, F. J. Castellino and D. P. Weliky, *J Am Chem Soc*, 2004, **126**, 14722-14723.
51. B. Apellaniz, E. Rujas, P. Carravilla, J. Requejo-Isidro, N. Huarte, C. Domene and J. L. Nieva, *J Virol*, 2014, **88**, 13367-13377.
52. H. Chakraborty and A. Chattopadhyay, *ACS Chem Neurosci*, 2015, **6**, 199-206.
53. S. Ganguly, A. H. Clayton and A. Chattopadhyay, *Biophys J*, 2011, **100**, 361-368.
54. R. Varma and S. Mayor, *Nature*, 1998, **394**, 798-801.
55. S.-T. Yang, A. J. B. Kreutzberger, J. Lee, V. Kiessling and L. K. Tamm, *Chemistry and Physics of Lipids*, 2016, **199**, 136-143.
56. G. Meher and H. Chakraborty, in *Human Viruses: Diseases, Treatments and Vaccines : The New Insights*, ed. S. I. Ahmad, Springer International Publishing, Cham, 2021, DOI: 10.1007/978-3-030-71165-8_33, pp. 693-712.
57. G. P. Pattnaik, G. Meher and H. Chakraborty, *Adv Exp Med Biol*, 2018, **1112**, 69-78.
58. P. T. Ivanova, D. S. Myers, S. B. Milne, J. L. McClaren, P. G. Thomas and H. A. Brown, *ACS Infectious Diseases*, 2015, **1**, 435-442.
59. R. Chan, P. D. Uchil, J. Jin, G. Shui, D. E. Ott, W. Mothes and M. R. Wenk, *J Virol*, 2008, **82**, 11228-11238.
60. R. C. Aloia, H. Tian and F. C. Jensen, *Proc Natl Acad Sci U S A*, 1993, **90**, 5181-5185.
61. R. D. Kaiser and E. London, *Biochemistry*, 1998, **37**, 8180-8190.
62. L. K. Tamm, X. Han, Y. Li and A. L. Lai, *Biopolymers*, 2002, **66**, 249-260.

63. C. Gray, S. A. Tatulian, S. A. Wharton and L. K. Tamm, *Biophysical Journal*, 1996, **70**, 2275-2286.
64. H. Chakraborty, T. Sengupta and B. R. Lentz, *Biophys J*, 2014, **107**, 1327-1338.
65. H. Chakraborty, P. K. Tarafdar, M. J. Bruno, T. Sengupta and B. R. Lentz, *Biophys J*, 2012, **102**, 2751-2760.
66. H. Chakraborty, P. K. Tarafdar, D. G. Klapper and B. R. Lentz, *Biophys J*, 2013, **105**, 2495-2506.
67. A. Joardar, G. P. Pattnaik and H. Chakraborty, *The Journal of Physical Chemistry B*, 2021, **125**, 13192-13202.
68. T. Sengupta, H. Chakraborty and Barry R. Lentz, *Biophysical Journal*, 2014, **107**, 1318-1326.
69. M. E. Haque, H. Chakraborty, T. Koklic, H. Komatsu, P. H. Axelsen and B. R. Lentz, *Biophys J*, 2011, **101**, 1095-1104.
70. M. E. Haque, A. J. McCoy, J. Glenn, J. Lee and B. R. Lentz, *Biochemistry*, 2001, **40**, 14243-14251.
71. H. Chakraborty, P. K. Tarafdar, D. G. Klapper and B. R. Lentz, *Biophys. J.*, 2013, **105**, 2495-2506.
72. D. C. Wiley and J. J. Skehel, *Annu Rev Biochem*, 1987, **56**, 365-394.
73. R. M. DuBois, H. Zaraket, M. Reddivari, R. J. Heath, S. W. White and C. J. Russell, *PLoS pathogens*, 2011, **7**, e1002398.
74. V. Buzon, G. Natrajan, D. Schibli, F. Campelo, M. M. Kozlov and W. Weissenhorn, *PLoS pathogens*, 2010, **6**, e1000880.
75. A. C. Walls, Y. J. Park, M. A. Tortorici, A. Wall, A. T. McGuire and D. Veesler, *Cell*, 2020, **181**, 281-292.e286.